



# How well can persistent contrails be predicted? An update

Sina Hofer<sup>1</sup>, Klaus Gierens<sup>1</sup>, and Susanne Rohs<sup>2</sup>

<sup>1</sup>Institut für Physik der Atmosphäre, Deutsches Zentrum für Luft- und Raumfahrt, Oberpfaffenhofen, Germany

<sup>2</sup>Forschungszentrum Jülich, IEK-8, Jülich, Germany

**Correspondence:** Sina Hofer (sina.hofer@dlr.de)

Received: 9 February 2024 – Discussion started: 28 February 2024

Revised: 15 May 2024 – Accepted: 22 May 2024 – Published: 11 July 2024

**Abstract.** The total aviation effective radiative forcing is dominated by non-CO<sub>2</sub> effects. The largest contributors to the non-CO<sub>2</sub> effects are contrails and contrail cirrus. There is the possibility of reducing the climate effect of aviation by avoiding flying through ice-supersaturated regions (ISSRs), where contrails can last for hours (so-called persistent contrails). Therefore, a precise prediction of the specific location and time of these regions is needed. But a prediction of the frequency and degree of ice supersaturation (ISS) on cruise altitudes is currently very challenging and associated with great uncertainties because of the strong variability in the water vapour field, the low number of humidity measurements at the air traffic altitude, and the oversimplified parameterisations of cloud physics in weather models.

Since ISS is more common in some dynamical regimes than in others, the aim of this study is to find variables/proxies that are related to the formation of ISSRs and to use these in a regression method to predict persistent contrails. To find the best-suited proxies for regressions, we use various methods of information theory. These include the log-likelihood ratios, known from Bayes' theorem, a modified form of the Kullback–Leibler divergence, and mutual information. The variables (the relative humidity with respect to ice,  $RH_{i_{ERA5}}$ ; the temperature,  $T$ ; the vertical velocity,  $\omega$ ; the divergence,  $DIV$ ; the relative vorticity,  $\zeta$ ; the potential vorticity,  $PV$ ; the normalised geopotential height,  $Z$ ; and the local lapse rate,  $\gamma$ ) come from ERA5, and  $RH_{M/I}$ , which we assume as the truth, comes from MOZAIC/IAGOS (Measurement of Ozone and Water Vapour on Airbus In-service Aircraft/In-service Aircraft for a Global Observing System; commercial aircraft measurements).

It turns out that  $RH_{i_{ERA5}}$  is the most important predictor of ice supersaturation, in spite of its weaknesses, and all other variables do not help much to achieve better results. Without  $RH_{i_{ERA5}}$ , a regression to predict ISSRs is not successful. Certain modifications of  $RH_{i_{ERA5}}$  before the regression (as suggested in recent papers) do not lead to improvements of ISSR prediction. Applying a sensitivity study with artificially modified  $RH_{i_{ERA5}}$  distributions points to the origin of the problems with the regression: the conditional distributions of  $RH_{i_{ERA5}}$  (conditioned on ISS and non-ISS, from  $RH_{M/I}$ ) overlap too heavily in the range of 70 %–100 %, so for any case in that range, it is not clear whether it belongs to an ISSR or not. Evidently, this renders the prediction of contrail persistence very difficult.

## 1 Introduction

In order to avoid persistent (warming) contrails, it is necessary that they can be reliably predicted. For this aim, three conditions need to be fulfilled. First, the formation of contrails has to be predicted with reasonable skill. Contrails form if (super)saturation with respect to water occurs during the mixing process of the ambient air with the exhaust gases from the aircraft. This criterion is called the Schmidt–Appleman criterion (SAC; see Schmidt, 1941; Appleman, 1953; Schumann, 1996). Second, contrails need ice supersaturation (ISS) to be persistent. So, this state must be represented and reliably predicted in weather models. Third, in order to determine whether a contrail will be warming or cooling in advance, some kind of radiative transfer calculation or a corresponding regression formula (e.g. Corti and Peter, 2009; Schumann et al., 2012; Wolf et al., 2023a) is required.

While the first of these conditions, the ability to predict the SAC, is generally fulfilled with a satisfying quality, this is not the case for the prediction of ice supersaturation (Gierens et al., 2020). Predicting ice supersaturation at air traffic cruise levels presents major difficulties. Gierens et al. (2020) compared temperature and humidity data obtained from instrumented passenger aircraft with reanalysis data interpolated in space and time to the measurement locations. They came to the result that the forecast of ice supersaturation at given times and locations (for flight routing purposes) is currently almost like tossing a coin. In contrast, the forecast of ISS is much easier for larger regions and periods of time (e.g. for planning measurement campaigns; see Voigt et al., 2017). In the present paper, we investigate the problem of the forecast of ISS in more detail and we do not cover the first and third condition.

There are several reasons why the prediction of persistent contrails is currently challenging. The main reason is the strong variability in the water vapour field in the atmosphere. This is because water substance is present in three aggregate states; it is involved in chemical and aerosol processes, and thus it varies greatly in the atmosphere. This problem is intensified by the low number of humidity measurements at cruise levels for data assimilation. Data assimilation is necessary to keep the simulation of a complex system close to measured reality. Therefore, more data on relative humidity at flight levels are urgently needed. Note that satellite data cannot fill this gap since their vertical resolution is insufficient (Gierens and Eleftheratos, 2020). A third reason for the challenging prediction of persistent contrails is that current parameterisations of ice cloud physics in weather models are generally kept simple enough in order not to spend too much computing time for a part of the atmosphere that so far has usually not been the main focus of weather prediction. ISS hardly affects the weather on the ground. Thus, it was not represented in numerical weather prediction (NWP) models until about 25 years ago (Wilson and Ballard, 1999; Tompkins et al., 2007), and its representation is still generally too

crude for a reliable prediction of ice supersaturation and contrail persistence.

However, there is growing interest in reducing the climate impact of aviation nowadays, and a relatively straightforward possibility would be the avoidance of the formation of persistent contrails if only ice supersaturation could be predicted with the precision necessary for flight routing. Because of the challenges mentioned before, the relative humidity field is insufficient for this purpose, and we need either corrections to the humidity field (Teoh et al., 2020, 2022) or other quantities that help in predicting of ISS. Gierens and Brinkop (2012) and Wilhelm et al. (2022) show that ISS is typically related to certain dynamical regimes, e.g. anticyclonic divergent uplift. This triggered the idea that using dynamical fields can indeed help in contrail forecast. We pursue this idea in the present study and show how far we can get with dynamical proxies together with modern regression methods. The results turn out to be considerably better than without such methods, but they are still not satisfying. A sensitivity study shows what impedes better results and where the source of the problem lies.

In the present paper, we concentrate on the prediction of ice supersaturation, i.e. the prediction of persistent contrails. For this purpose, we use data obtained from an instrumented passenger aircraft and reanalysis data, which are explained in Sect. 2. We test different methods for predicting persistent contrails, which is the content of Sect. 3, as well as the results we obtained. Later on, in Sect. 4, we concentrate on modifying the relative humidity of ERA5 and on different sensitivity tests to artificially separate the conditional  $RH_i$  distributions of ERA5. Finally, we summarise our results and conclude in Sect. 5.

## 2 Data

Various data sources are utilised in this study. These are briefly described in the following sections, Sect. 2.1 and 2.2.

### 2.1 Data from a commercial aircraft

In this study, we use pressure and relative humidity with respect to ice ( $RH_{M/I}$ ) data collected from 16 588 flights during 10 years (2000–2009) of MOZAIC (Measurement of Ozone and Water Vapour on Airbus In-service Aircraft; Marenco et al., 1998) measurements. As MOZAIC was transferred to the European infrastructure IAGOS (In-service Aircraft for a Global Observing System; Petzold et al., 2015) in 2011, we refer to the data as MOZAIC/IAGOS (<https://www.iagos.org>, last access: 4 July 2024). MOZAIC/IAGOS operates autonomous in situ instruments installed on a long-range commercial aircraft. Due to this, it has the highest data density in the flight corridors of the mid-latitudes, making it an ideal data set for the investigation of contrail-forming regions. MOZAIC/IAGOS in situ measurements are available every 4 s. This corresponds to a flight distance of around

1 km. We randomly select only 1 % of the data points (around every 100th point) to avoid autocorrelation. This means the temporal distance is around 400 s on average.

For this study, we have chosen aerial boundaries of 30 to 70° latitude and –125 to 145° longitude at cruise levels between 310 and 190 hPa, that is, a region with heavy air traffic. We use these data as a basic truth to determine whether the formation of a persistent contrail is possible or not at a specific position and time.

## 2.2 Reanalysis data

In addition to the data from commercial aircraft, hourly ERA5 high-resolution realisation (HRES) reanalysis data (Hersbach et al., 2018a, b, 2020) of the relative humidity with respect to ice,  $RH_{iERA5}$ ; the temperature,  $T$ ; the vertical velocity,  $\omega$ ; the divergence,  $DIV$ ; the relative vorticity,  $\zeta$ ; the potential vorticity,  $PV$ ; and the normalised geopotential height,  $Z$ , for 200, 225, 250, and 300 hPa from the Copernicus Data Service (Copernicus Climate Change Service, 2017) of ECMWF (European Centre for Medium-Range Weather Forecast) are retrieved and interpolated to the exact position and time of the aircraft (see ERA5, <https://cds.climate.copernicus.eu>, last access: 4 July 2024). The chosen pressure range from 300 to 200 hPa covers approximately the flight levels of 300 to 390 hft (hectofeet; 100 ft corresponds to approximately 30 m). The spatial resolution of these data is  $1^\circ \times 1^\circ$ . With the pressure and temperatures on two adjacent levels, the local lapse rate,  $\gamma$ , at the aircraft positions is also calculated (Gierens et al., 2022). The selection of these particular variables comes from Wilhelm et al. (2022).

## 3 Methods and results

In this work, we consider whether it is possible to use the dynamical proxies suggested by Wilhelm et al. (2022) to improve the forecast of ice supersaturation and contrail persistence. To quantify the success (or not) of several approaches we took, we use the equitable thread score (ETS) as in Gierens et al. (2020). The motivation for this choice of score value, the defining equations, and interpretation of the ETS are given below in Sect. 3.2.3.

The most simple way to map the values of the six dynamical proxies to probabilities for ice supersaturation or contrail persistence is to divide the phase space into six-dimensional rectangles/blocks (six because of the six suggested dynamical proxies by Wilhelm et al., 2022), to count the number of cases with persistent contrails in each block, and to divide it by the total amount of data in that block. The blocks should not be too large so that the probabilities are specific for certain circumstances. Simultaneously, the blocks must not be too small so that the number of events in each block allows one to determine the probability with some statistical reliability. Unfortunately, it turns out that even almost 400 000

data points are insufficient for this simple and most straightforward method; many blocks are either empty or do not have enough data points unless we use quite large blocks and lose precision. Therefore, we cannot use this simple method and have to try others, like Bayesian learning or modern non-linear regression methods.

## 3.1 Bayesian learning

### 3.1.1 Theory

We are interested in whether persistent contrails are possible or not, i.e. whether there is ice supersaturation or not. Unfortunately, the moisture field in the models is not accurate enough for that purpose. So, how can we solve this problem?

It is known that ISS is more frequent in some dynamic situations than in others (Gierens and Brinkop, 2012; Gierens et al., 2022; Wilhelm et al., 2022). One can try to exploit the fact that there are certain dynamical quantities,  $X$ , whose conditional probability densities,  $f_X(x|ISS)$  and  $f_X(x|\overline{ISS})$ , differ more or less from each other (read as  $f_X(x|ISS)$  being the probability density for a quantity  $X$  for the special value  $x$  in cases where ISS prevails;  $f_X(x|\overline{ISS})$  is the analogue for cases where non-ISS ( $\overline{ISS}$ ) prevails).

Let us assume there is a value  $x$  of a variable  $X$  and that this particular value is compatible with both ISS and  $\overline{ISS}$ . Then the question arises of which statements can be made about ice supersaturation using this quantity. Is it more likely or less likely when  $X = x$ ?

Naively, one could compare  $f_X(x|ISS)$  and  $f_X(x|\overline{ISS})$  and choose the larger of the two values. However, this ignores the fact that  $\overline{ISS}$  cases are much more frequent than ISS cases when no further circumstances are considered – the so-called a priori probability. The latter is taken into account by Bayes' theorem in the following form:

$$P(ISS|X = x) = \frac{P(x|ISS) \cdot P(ISS)}{P(x|ISS) \cdot P(ISS) + P(x|\overline{ISS}) \cdot P(\overline{ISS})}, \quad (1)$$

where  $P(ISS)$  is the a priori probability for ice supersaturation.  $P(x|ISS) = \int f_X(x|ISS) dx$  and  $P(x|\overline{ISS}) = \int f_X(x|\overline{ISS}) dx$ . In Eq. (1), the  $dx$  is cancelled out and, on the right side of the equation,  $P(x|ISS)$  and  $P(x|\overline{ISS})$  can be replaced by the corresponding densities,  $f_X(x|ISS)$  and  $f_X(x|\overline{ISS})$ .

Another possibility of framing Bayes' theorem for the present problem is to use an odds ratio:

$$\frac{P(ISS|x)}{P(\overline{ISS}|x)} = \frac{f_X(x|ISS)}{f_X(x|\overline{ISS})} \cdot \frac{P(ISS)}{P(\overline{ISS})}. \quad (2)$$

The first factor on the right side of Eq. (2) is the likelihood ratio, which represents the gain ( $> 1$ ) or loss ( $< 1$ ) in confidence for ISS that we get by learning the current value of  $X$ . A likelihood ratio exceeding 1 does not mean that ISS is more likely than  $\overline{ISS}$  but that the probability of ISS increases. ISS is only more likely than  $\overline{ISS}$  if the factor on the

left side, the a posteriori odds ratio, is larger than 1. The second factor on the right side is the prior odds ratio. In our case,  $P(\text{ISS})$  is given by the ratio of the number of data points with ISS and the total number of data points (according to MOZAIC/IAGOS), which is 0.125. So, only 12.5 % of our data belong to the ISS class. The prior odds ratio is therefore  $0.125/0.875 \approx 0.14$ . This means that the likelihood ratio has to be larger than  $1.0/0.14 = 7.14$  to make ISS more probable than  $\overline{\text{ISS}}$ . Instead of the odds ratio, one often uses its logarithm, which leads to log-likelihood ratios (also known as logits) with values symmetric around 0 (instead of values asymmetric around 1). That is, positive logits increase the probability for ISS and negative logits decrease the probability for ISS. As mentioned before, the a posteriori odds ratio has to be larger than 1 to make ISS more probable than  $\overline{\text{ISS}}$ . This also means that the logarithm of the a posteriori ratio has to be positive to make ISS more likely than  $\overline{\text{ISS}}$ . As the logarithm of the prior odds ratio is  $\ln(0.125/(1 - 0.125)) \approx -2$ , the logit must exceed 2 to make ISS more probable than  $\overline{\text{ISS}}$ .

As long as there is only one special value  $x$  of a dynamical variable  $X$ , we are finished and this is already the result. Now, assume that there are two quantities,  $X$  and  $Y$ , and one wants to know which of these quantities carries more information about the probability of ice supersaturation. Obviously, it is the quantity whose logits deviate more from zero in both the positive and negative directions or the quantity for which the absolute values of the logits are larger on average over the ranges of  $x$  and  $y$ . Taking the averages has to be done with a weighting that accounts for the values of the variables that actually occur in a given situation, e.g.

$$E_{\text{AL}}(f_{X|\text{ISS}}||f_{X|\overline{\text{ISS}}}) = \int f_X(x|\text{ISS}) \cdot \left| \ln \left( \frac{f_X(x|\text{ISS})}{f_X(x|\overline{\text{ISS}})} \right) \right| dx. \quad (3)$$

As one does not know in advance whether a situation is ISS or not, it is best to also use the corresponding expectation of the absolute logit,  $E_{\text{AL}}(f_{X|\overline{\text{ISS}}}|f_{X|\text{ISS}})$  (where ISS and  $\overline{\text{ISS}}$  are interchanged), and to average the two results. Let the result for  $X$  be  $E_{\text{AL}}(X)$ . It may be called the expectation of the absolute logit. The quantity that yields the largest  $E_{\text{AL}}(X)$  has the largest learning effect for the question of whether a situation is ISS or not.

Note that  $E_{\text{AL}}(|\cdot|)$  has some resemblance to a quantity known as Kullback–Leibler divergence,  $D_{\text{KL}}(f_{X|\text{ISS}}||f_{X|\overline{\text{ISS}}})$  (the same expression without the absolute sign), and the corresponding symmetric form (the mean value of the two asymmetrical divergences,  $D_{\text{KL}}(f_{X|\text{ISS}}||f_{X|\overline{\text{ISS}}})$  and  $D_{\text{KL}}(f_{X|\overline{\text{ISS}}}|f_{X|\text{ISS}})$ ) is known as Jeffreys divergence in information theory. For quantities that are not related to supersaturation,  $f_X(x|\text{ISS}) = f_X(x|\overline{\text{ISS}}) = f_X(x)$ , and the logit is zero. Thus,  $E_{\text{AL}}(X) = 0$  as well, which signifies that one cannot learn anything about the presence of ISS using such a quantity.

### 3.1.2 Application

The conditional probability densities of the dynamical proxies of ERA5 for ISS and  $\overline{\text{ISS}}$  cases (depending on whether the relative humidity with respect to ice of MOZAIC/IAGOS,  $\text{RH}_{i\text{M/I}}$ , is  $\geq 1.0$  or  $< 1.0$ ) are calculated using the Epanechnikov smoothing kernel with 300 equally spaced points between the minimum and maximum of the respective proxy. The log-likelihood ratios for some dynamical quantities are shown in Fig. 1. ISS gains in probability are relative to the low prior probability if the log-likelihood ratio is positive and vice versa (solid line in the diagrams). However, it needs to exceed 2 to make ISS more probable than  $\overline{\text{ISS}}$  (dashed lines). Obviously, this threshold is only exceeded in quite small ranges of the proxies or not at all. Only where  $\text{RH}_i$  from ERA5 exceeds 100 % does the logit exceed 2; this says that ISS and persistent contrails are more probable than not (the wiggles in the curve at even higher  $\text{RH}_i$  are considered noise). The low values of the logits of the other variables indicate that the dynamical proxies do not help much in predicting ice supersaturation via the Bayesian law. Obviously, the strong separation of their conditional distributions is only a necessary but not a sufficient condition for good proxies.

For the calculation of the expectation of the absolute logit  $E_{\text{AL}}(X)$  (see Eq. 3), the absolute values of the different logit functions are needed. These are shown in orange in Fig. 2 for different proxies. The products of these functions with either of the conditional densities are shown as well in light blue and dark purple. The integrals of these functions are given in Table 1 for the relative humidity with respect to ice,  $\text{RH}_{i\text{ERA5}}$ ; the temperature,  $T$ ; the vertical velocity,  $\omega$ ; the divergence,  $\text{DIV}$ ; the relative vorticity,  $\zeta$ ; the potential vorticity,  $\text{PV}$ ; the lapse rate,  $\gamma$ ; and the normalised geopotential height,  $Z$ . The averages of the first two rows of each column are the desired  $E_{\text{AL}}(X)$ . High values for  $\text{RH}_{i\text{ERA5}}$ ,  $\zeta$ , and  $\gamma$  are noticeable for the ISS case and high values for  $\text{RH}_{i\text{ERA5}}$ ,  $\text{PV}$ , and  $\gamma$  for  $\overline{\text{ISS}}$ . Therefore, according to our analysis,  $\text{RH}_{i\text{ERA5}}$ ,  $\zeta$ ,  $\gamma$ , and  $\text{PV}$  seem to be the best-suited proxies for our purpose, but, as stated, they should be tried rather for regression and not for Bayesian learning. The high value of  $E_{\text{AL}}(\text{PV})$  is probably due to the fact that a high  $\text{PV}$  indicates the stratosphere where ISS hardly occurs. So, for tropospheric situations (low- $\text{PV}$  cases), this finding is not very helpful, and, accordingly, the high  $E_{\text{AL}}(\text{PV})$  must not be over-interpreted.

To apply the Bayesian law for several proxies simultaneously, e.g. as for  $P(\text{ISS}|\text{RH}_{i\text{ERA5}}, \zeta, \gamma)$ , we would need a much larger amount of data to compute the likelihood ratios with some robustness over the whole domain. Instead, we now try to apply non-linear regression.

### 3.2 Non-linear regression

The dynamical candidate proxies are not independent quantities, and one has to take care that a regression is not formu-

**Table 1.** Expectation values for absolute logit of the different proxies.  $E_{AL}(X)$  is the mean of  $E_{AL}(f_{X|ISS}\|f_{X|\overline{ISS}})$  and  $E_{AL}(f_{X|\overline{ISS}}\|f_{X|ISS})$ , so  $E_{AL}(X) = \frac{1}{2} \cdot (E_{AL}(f_{X|ISS}\|f_{X|\overline{ISS}}) + E_{AL}(f_{X|\overline{ISS}}\|f_{X|ISS}))$ .

Quantity	$RH_{iERA5}$	$T$	$\omega$	DIV	$\zeta$	PV	$\gamma$	$Z$
$E_{AL}(f_{X ISS}\ f_{X \overline{ISS}})$	1.75	0.34	0.56	0.42	0.96	0.90	0.96	0.52
$E_{AL}(f_{X \overline{ISS}}\ f_{X ISS})$	3.41	0.38	0.43	0.33	1.20	2.07	1.24	0.88
$E_{AL}(X)$	2.58	0.36	0.50	0.38	1.08	1.49	1.10	0.70

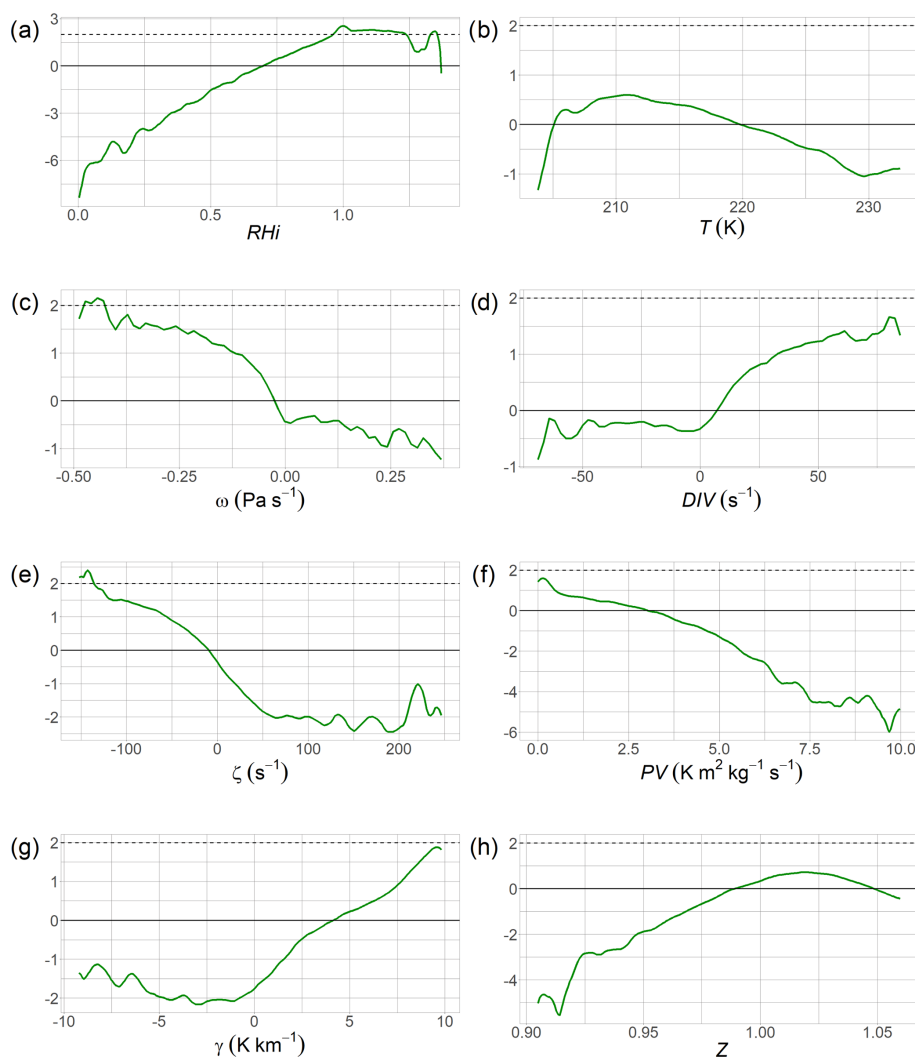


**Figure 1.** Log-likelihood ratios for dynamical quantities. Positive values raise the probability for ISS and negative values lower it. The probability for ISS exceeds the probability for  $\overline{ISS}$  only in the small ranges where the log likelihood reaches values above 2 (marked by the dashed lines).

lated with redundant information. But, of course, a variable that has some relation with (i.e. information on) the relative humidity is welcome. Above, we see that  $RH_{iERA5}$ ,  $\zeta$ , and  $\gamma$  are promising in this respect. Also, PV has a quite large absolute logit, but that comes mainly from the  $\overline{ISS}$  cases, where it is an expression of the fact that dry stratospheric

air (with  $PV > 3.5$ ) is rarely found in a supersaturated state (Neis, 2017; Petzold et al., 2020). Here, we apply another measure. Usually, one uses the linear correlation between the input data, but this does not work if the quantities are related in a non-linear fashion. Therefore, it is necessary to use a

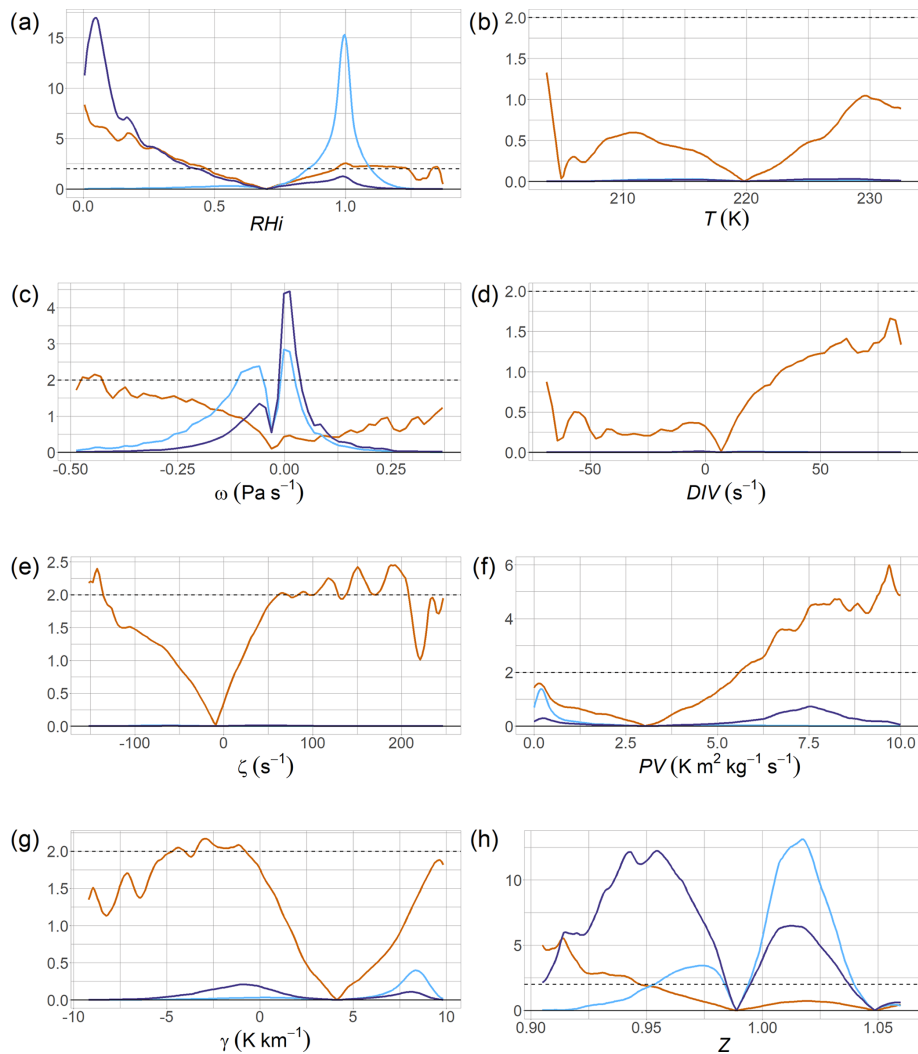


**Figure 2.** The absolute logarithm of the quotient of the densities for ISS and  $\overline{\text{ISS}}$  cases (orange), the absolute logarithm of the quotient of the densities for ISS and  $\overline{\text{ISS}}$  cases multiplied by the density for ISS cases (light blue), and the absolute logarithm of the quotient of the densities for  $\overline{\text{ISS}}$  and ISS cases multiplied by the density for  $\overline{\text{ISS}}$  cases (dark purple) (see Eq. 3).

more general measure of correlation, namely the mutual information from information theory.

### 3.2.1 Mutual information

The mutual information is a measure of information that one variable,  $X$ , can provide about another,  $Y$ . Its formulation uses the joint distribution of  $X$  and  $Y$  and both marginal distributions:

$$I(X; Y) = \int \int f_{X \cap Y}(x, y) \cdot \log \left( \frac{f_{X \cap Y}(x, y)}{f_X(x) \cdot f_Y(y)} \right) dx dy, \quad (4)$$

where  $f_{X \cap Y}(x, y)$  is the joint probability density for  $X$  and  $Y$ . In the case that  $X$  and  $Y$  are independent, the joint density equals the product of the marginal densities and the logarithm is zero. Then, the mutual information between  $X$  and  $Y$  is zero as well. In all other cases, it is positive and it is the

expected value of  $\log \left( \frac{f_{X \cap Y}}{f_X f_Y} \right)$  with the joint distribution as the weight function.

Since we assume the humidity of MOZAIC/IAGOS ( $RHi_{M/I}$ ) is the truth, we calculate the mutual information of  $RHi_{M/I}$  with other quantities and compare them with each other. The results of the computed mutual information  $I(RHi_{M/I}; Y)$  for different variables  $Y$  are shown in the first row in Table 2. The highest values of the mutual information are reached by  $RHi_{ERA5}$  (1.26 bits),  $PV$  (0.57 bits),  $\gamma$  (0.38 bits), and  $\zeta$  (0.37 bits). This means, according to the mutual information, that  $RHi_{ERA5}$ ,  $PV$ ,  $\gamma$ , and  $\zeta$  seem well suited as proxies for regressions.

To be a good proxy for a regression, it must not only be well correlated with  $RHi_{M/I}$  (i.e. have a high value of mutual information,  $I(RHi_{M/I}; Y)$ ), but, at the same time, it should not be correlated with other variables (i.e. a low value of mu-

tual information with the other proxies,  $I(X; Y)$ ) to avoid redundant information. The values of the individual mutual information,  $I(X; Y)$ , can be found on the right side in Table 2. The matrix is symmetrical, so, for a better overview, only one side is filled.

As mentioned before, out of all quantities,  $RHi_{ERA5}$ , PV,  $\gamma$ , and  $\zeta$  have the highest mutual information with  $RHi_{M/I}$ . However, PV and  $\gamma$  are themselves quite strongly correlated (1.07 bits). So, because  $I(RHi_{M/I}; PV) > I(RHi_{M/I}; \zeta)$  but  $I(PV; \zeta)$  is also very high,  $\zeta$  should be omitted when using PV as a proxy.

### 3.2.2 Generalised additive model

A generalised additive model (GAM) is a regression method for predicting a response  $Y$  based on non-linear functions of several predictors,  $X = \{X_1, X_2, \dots, X_p\}$ . In meteorology, for instance, it has been successfully used for the prediction of thunderstorms (Rädler et al., 2018). The general formula for GAMs is

$$\log\left(\frac{P(\text{ISS}|X)}{1 - P(\text{ISS}|X)}\right) = \beta_0 + s_1(X_1) + s_2(X_2) + \dots + s_p(X_p). \quad (5)$$

$\frac{P(\text{ISS}|X)}{1 - P(\text{ISS}|X)}$  is the posterior odds ratio,  $P(\text{ISS}|X)/P(\overline{\text{ISS}}|X)$ . The GAM thus constructs a relation between the (posterior) odds ratio and a linear combination of functions of the set of predictors,  $X$ . For the functions, we use smoothing splines,  $s(X)$ . Here, we test the following six different GAMs with combinations of various dynamical proxies (input parameters) to predict whether persistent contrails are possible:

- GAM<sub>0</sub> with  $RHi_{ERA5}$ ,
- GAM<sub>1</sub> with  $T$ ,  $RHi_{ERA5}$ ,
- GAM<sub>2</sub> with PV,  $T$ ,  $RHi_{ERA5}$ ,
- GAM<sub>3</sub> with PV,  $T$ ,  $\zeta$ ,  $RHi_{ERA5}$ ,
- GAM<sub>4</sub> with  $\gamma$ ,  $T$ , Z, PV,  $\zeta$ , and
- GAM<sub>5</sub> with  $\gamma$ ,  $T$ , Z, PV,  $\zeta$ ,  $RHi_{ERA5}$ .

The procedure is as follows: for the tests, 395 576 independent data points are used. First, we divide the data set (MOZAIC/IAGOS and ERA5 data) into a training and test data set (training data set makes up  $\sim 80\%$  and test data set  $\sim 20\%$  of the whole data set). The presence of persistent contrails is known from the MOZAIC/IAGOS data, as described in Sect. 2.1. Next, we train the model, which means that we find the best coefficients for the relationships between the proxies and prediction using the training data set and a software environment for statistical computing called R (Ihaka and Gentleman, 1993). Then, we use the gained best coefficients and functions to predict the presence of persistent contrails in the test data set. At the end, we validate the forecast by comparing the predictions with the truth and calculating the so-called equitable threat score (see Sect. 3.2.3).

### 3.2.3 Equitable threat score

In this study, the equitable threat score (ETS) is used to validate and compare the prediction accuracy of the different GAMs (with varied input parameters) with that of the raw data. For the calculation of the ETS (Gierens et al., 2020), the events are summed up according to the contingency table (see Table 3), where a distinction is made between potential persistent contrails predicted (yes or no) and persistent contrails observed (yes or no).

The sum of the events is labelled as  $a$  (contrails are predicted and observed),  $b$  (no contrails are predicted but observed),  $c$  (contrails are predicted but not observed), and  $d$  (contrails are neither predicted nor observed). For the calculation of the ETS, the numbers of the events,  $a$ ,  $b$ ,  $c$ , and  $d$ , and the following equation are used:

$$\text{ETS} = \frac{a - r}{a + b + c - r}, \quad (6)$$

with

$$r = \frac{(a + b) \cdot (a + c)}{a + b + c + d}. \quad (7)$$

If the prediction agrees perfectly with the observation,  $\text{ETS} = 1$ . For a completely inverse relation, ETS is negative, and for a random relation,  $\text{ETS} = 0$ . The advantage of using ETS instead of another skill score is that the influence of the predominant case in which ISS is neither predicted nor observed (large value of  $d$ ) is minimised. This is the case here, since  $\overline{\text{ISS}}$  is much more probable than ISS.

In order to fill the contingency table, it is necessary to decide on a conditional probability threshold  $P(\text{ISS}|X)$  up to which  $\overline{\text{ISS}}$  and from which ISS is predicted. To determine the threshold, one generally uses the value that gives the best ETS. In the present case, this threshold probability is 0.34. That is, with a given set of proxies,  $X$ , we predict contrail persistence or ice supersaturation if  $P(\text{ISS}|X) > 0.34$  (and vice versa).

### 3.2.4 Regression results

Table 4 shows the results of the application of six different general additive models (GAM<sub>0</sub> to GAM<sub>5</sub>). Note that  $\beta_0$  is different for every GAM even if it is abbreviated in the same way in all GAMs. In the first (white) row, the ETS value of 0.198 is given, which is obtained when only  $RHi_{ERA5}$  and  $RHi_{M/I}$  are compared (without applying a GAM to it). In that case, we only check how well the prediction of ISS in ERA5 matches the observation of ISS of MOZAIC/IAGOS. So, it is only examined how often  $RHi_{ERA5} \geq 1.0$  matches  $RHi_{M/I} \geq 1.0$ . The SAC is not taken into account.

In GAM<sub>0</sub>, we only use  $RHi_{ERA5}$  and get an ETS value of 0.337. In GAM<sub>1</sub>, we also take  $T$  into account since the temperature and the humidity are the two important variables

**Table 2.** The mutual information matrix,  $I(X; Y)$ , is used to identify the correlations of the variables with each other. The first row of the matrix,  $I(\text{RH}_{M/I}; Y)$ , shows the correlation of  $\text{RH}_{M/I}$  with the other proxies and the columns the correlations between the variables among themselves.

$I(X; Y)$ in bits	$\text{RH}_{M/I}$	$\text{RH}_{\text{ERA5}}$	$T$	$\omega$	DIV	$\zeta$	PV	$\gamma$	$Z$
$\text{RH}_{M/I}$		1.26	0.29	0.06	0.04	0.37	0.57	0.38	0.23
$\text{RH}_{\text{ERA5}}$			0.35	0.08	0.06	0.43	0.61	0.43	0.25
$T$				0.02	0.02	0.12	0.16	0.05	0.36
$\omega$					0.21	0.04	0.09	0.10	0.06
DIV						0.03	0.04	0.04	0.03
$\zeta$							0.73	0.43	0.19
PV								1.07	0.54
$\gamma$									0.54
$Z$									

**Table 3.** Contingency table for predicting and observing persistent contrails.

		Potential persistent contrails predicted	
		Yes	No
Persistent contrails observed	Yes	correct ( <i>a</i> )	false negative ( <i>b</i> )
	No	false positive ( <i>c</i> )	correct ( <i>d</i> )

to compute whether contrails form (using the SAC). With these proxies we get an ETS of 0.372, which is a little bit higher than in  $\text{GAM}_0$  but not significantly.

As we saw in Sect. 3.2.1, when calculating the mutual information,  $\text{RH}_{\text{ERA5}}$ , PV,  $\zeta$ , and  $\gamma$  show particularly high values with  $\text{RH}_{M/I}$  ( $I(\text{RH}_{M/I}; \text{RH}_{\text{ERA5}}) = 1.26$  bits,  $I(\text{RH}_{M/I}; \text{PV}) = 0.57$  bits,  $I(\text{RH}_{M/I}; \gamma) = 0.38$  bits, and  $I(\text{RH}_{M/I}; \zeta) = 0.37$  bits) and are therefore very suitable as proxies. But when looking at the mutual information among these proxies, then it is noticeable that in particular PV and  $\gamma$  correlate strongly (1.07 bits). That is why  $\gamma$  can be omitted when using PV.  $I(\text{PV}; \zeta)$  is also very high (0.73 bits), which is why we only use the PV in  $\text{GAM}_2$  (in addition to  $T$  and  $\text{RH}_{\text{ERA5}}$ ). The resulting ETS value is also 0.372.

For  $\text{GAM}_3$ , we use PV,  $T$ ,  $\zeta$ , and  $\text{RH}_{\text{ERA5}}$  because we want to enter even more proxies in the GAM as inputs according to the mutual information. So, we do the same GAM as before, but we also use  $\zeta$  because  $I(\text{RH}_{M/I}; \zeta)$  is also very high and  $I(\text{PV}; \zeta) < I(\text{PV}; \gamma)$ . The ETS in this case is 0.373. We see that  $\text{GAM}_2$  and  $\text{GAM}_3$  hardly differ from  $\text{GAM}_1$  in terms of their ETS values. The reason for this is that even if  $I(\text{RH}_{M/I}; \text{PV})$  is very high, the PV is already very strongly correlated with  $\text{RH}_{\text{ERA5}}$  ( $I(\text{RH}_{\text{ERA5}}; \text{PV}) = 0.61$  bits). This means that not much more additional information is provided by PV (and the other variables provide even less).

Next, we use all proxies that show separate distributions in their probability density functions (PDFs, not shown),  $P(X|\text{ISS})$  vs.  $P(X|\bar{\text{ISS}})$ , but, as an experiment, we omit  $\text{RH}_{\text{ERA5}}$  in  $\text{GAM}_4$ . So, we use  $\gamma$ ,  $T$ ,  $Z$ , PV, and  $\zeta$  as inputs. The ETS only reaches a value of 0.197. This shows us two important things:

- i. Even if we supposedly put more information into the GAM using more proxies, the ETS does not increase.
- ii. The relative humidity cannot be ignored as an input variable. This indicates that even if the relative humidity is an imprecise variable, it must not be excluded; otherwise, the ETS value will drastically decrease.

These two new insights may be explained by the log-likelihood ratios (Fig. 1): only  $\text{RH}_{\text{ERA5}}$  shows values above 2 for a large range, so ISS is more probable in this range. This is probably the reason why  $\text{RH}_{\text{ERA5}}$  has to be used as an input for the GAMs. All other quantities show values above 2 either not at all or only for a very small range.

Using the same proxies as before and adding  $\text{RH}_{\text{ERA5}}$  ( $\text{GAM}_5$ ), the corresponding ETS reaches a value of 0.378.

It seems that the use of dynamical proxies in the GAMs does not outperform a simple GAM that uses only relative humidity and temperature by much. At least the ETS values obtained via the GAMs (that is, for prediction of potential persistent contrails) distinctively exceed those obtained from a simple check of the ISS prediction, as can be seen from the study of Gierens et al. (2020, in which  $\text{ETS} = 0.08$  for a relatively small set of data from 2014) and from the present much larger data set ( $\text{ETS} = 0.198$ ). This means that even if a value of 0.378 seems small at first glance, it is still larger than if the prediction of ice supersaturation is purely based on the relative humidity with respect to ice from the ERA5 data.

Note that despite  $T$  not being particularly prominent in neither the  $E_{\text{AL}}$  nor its mutual information with  $\text{RH}_{M/I}$ , we use it in  $\text{GAM}_1$  to  $\text{GAM}_5$  because it is such an important

quantity in the SAC, and we use the proxies to provide further information (in addition to  $T$  and  $\text{RH}_{i\text{ERA5}}$ ). So, when running our best GAM ( $\text{GAM}_5$ ), but this time without  $T$ , the ETS reaches a value of 0.357.  $T$  does not increase the ETS significantly, but we leave it in for the reasons mentioned above.

Since, as we have seen, the relative humidity should definitely be used as an input for a GAM, although it is not very precise, the questions arise of whether it is possible to improve the regression results using corrections to the relative humidity field from the weather forecast models and what the reason for why even the most advanced regression methods are not able to yield better ETS values is. These questions are dealt with in the next section.

#### 4 Sensitivity tests

If weather forecasts were perfect, contrail persistence could easily be predicted using temperature and relative humidity alone and it would not be necessary to use any proxies. Unfortunately, it seems that the predicted humidity field in particular (at least from ERA5 but certainly from other weather models as well) is not good enough to allow for such a forecast for single flights, that is, waypoint to waypoint (Gierens et al., 2020). There are plausible reasons for this, a lack of in situ observations of humidity at cruise levels and outdated cirrus parameterisations in numerical weather prediction models in particular (Sperber and Gierens, 2023). In the following, we perform regression tests with artificially changed distributions of relative humidity. We first assume that the two conditional  $\text{RH}_{i\text{ERA5}}$  distributions,  $P(\text{RH}_{i\text{ERA5}}|\text{ISS})$  and  $P(\text{RH}_{i\text{ERA5}}|\overline{\text{ISS}})$ , were more separated (less overlap) than they are (ideally the overlap should be very small, including only sublimating contrails in the ISS-conditioned PDF and cases that are supersaturated but too warm in the  $\overline{\text{ISS}}$ -conditioned PDF). Second, we test two different methods of humidity corrections to see whether they help to reach higher ETS values in the regression models.

##### 4.1 Separating the probability density functions conditioned on persistence

We guess that the root of the problem of predicting ice supersaturation and contrail persistence is the too strong of an overlap of the two conditional humidity PDFs, namely  $f_{\text{RH}_{i\text{ERA5}}}(r|\text{ISS})$  and  $f_{\text{RH}_{i\text{ERA5}}}(r|\overline{\text{ISS}})$ , where  $r$  is a special value of  $\text{RH}_{i\text{ERA5}}$ . This substantial overlap can be seen in panel (f) of Fig. 3. Now we artificially separate these two distributions using a perfectly separated pair of distributions, a log-normal distribution  $f_{\text{PC}}$ , cut off at 0.8 and 1.5 for cases that allow for persistent contrails (PC), and a second one,  $f_{\text{noPC}}$ , ranging from 0.0 and 0.8 for cases that do not (no PC). Then, we mix the original conditional probability distributions of all data, both in the training and test data set, more and more into the artificial distributions, namely using

a weighting factor,  $0 \leq a \leq 1$ , as follows:

$$\begin{aligned} f(r|\overline{\text{ISS}}, a) &= a f_{\text{noPC}} + (1 - a) f_{\text{RH}_{i\text{ERA5}}}(r|\overline{\text{ISS}}), \\ f(r|\text{ISS}, a) &= a f_{\text{PC}} + (1 - a) f_{\text{RH}_{i\text{ERA5}}}(r|\text{ISS}). \end{aligned} \quad (8)$$

Some examples of these artificial distributions are shown in Fig. 3. From these distributions, we draw random humidity values and replace the original ones with them, keeping their ISS and  $\overline{\text{ISS}}$  label (i.e. either persistent contrail,  $\text{RH}_{i\text{a}}$ , drawn from  $f(r|\text{ISS}, a)$  or non-persistent or no contrail drawn from  $f(r|\overline{\text{ISS}}, a)$ ). This data set is then again divided into a training (80 %) and test data (20 %) set and GAMs (with  $T$  and  $\text{RH}_{i\text{a}}$  like in  $\text{GAM}_1$ ) and the corresponding ETSs are computed for every value of  $a$ .

The results are shown in Table 5. It is noticeable that even with a small shift in the relative humidity data, the ETS value increases drastically. This can be observed especially for small values of  $a$ , which means that if the original  $\text{RH}_{i\text{ERA5}}$  data were just slightly more separated, the results would drastically improve. This is good news since it shows that the model prediction of  $\text{RH}_{i\text{ERA5}}$  does not need to be perfect. Very good ETS values already appear for conditional distributions that are a little less separated than they actually are. Note that the further increase in ETS of  $a > 0.5$  is quite weak since ETS ( $a = 0.5$ ) already exceeds 0.9.

##### 4.2 Correction formulas

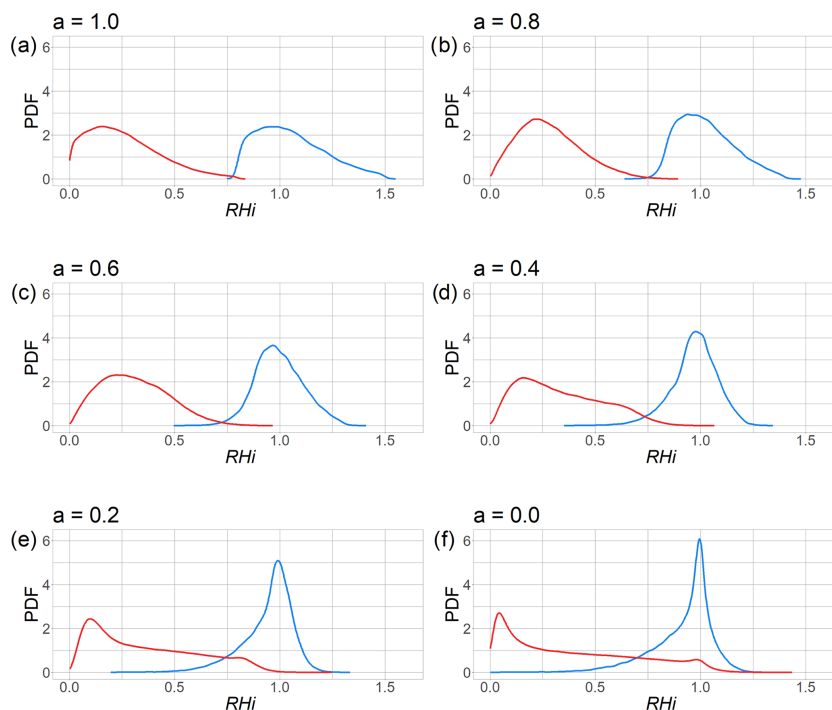
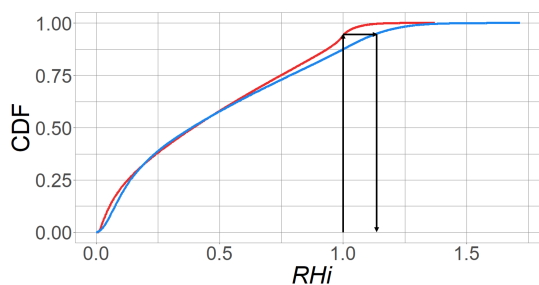
As Sect. 4.1 shows, there is a strong increase in the ETS for decreasing overlap. For this reason, two different methods are being tested to further separate the two conditional distributions,  $f_{\text{RH}_{i\text{ERA5}}}(r|\text{ISS})$  and  $f_{\text{RH}_{i\text{ERA5}}}(r|\overline{\text{ISS}})$ , using corrections to the modelled relative humidity values. These correction methods are quantile mapping based on the present data sets (e.g. Gierens and Eleftheratos, 2017; Wolf et al., 2023b) and the  $\text{RH}_i$  modification used by Teoh et al. (2022).

###### 4.2.1 Quantile mapping

The quantile mapping procedure uses the two cumulative distributions of  $\text{RH}_i$ , the one from the MOZAIC/IAGOS data and the corresponding one from ERA5; see Fig. 4. Evidently, the two distributions differ, in particular around saturation. This is, therefore, the range of values where corrections have the greatest effect. The procedure is quite simple: for each  $\text{RH}_{i\text{ERA5}}$ , the corresponding quantile value (the value on the  $y$  axis) is looked up and the corresponding  $\text{RH}_{i\text{M/I}}$  that has the same quantile value is taken as the corrected  $\text{RH}_{i\text{QM}}$ . This is illustrated by the black arrows in Fig. 4. We note that saturation ( $\text{RH}_{i\text{QM}} = 1$ ) is already reached at the predicted (i.e. ERA5) relative humidity of  $\text{RH}_{i\text{ERA5}} = 0.934$  using this method.

**Table 4.** Results of comparing  $RHi_{ERA5}$  and  $RHi_{M/I}$  with each other and of different GAMs.

Comparison of raw data (assessment of the ISS prediction without using a GAM)		ETS
$RHi_{ERA5}$ and $RHi_{M/I}$		0.198
Prediction of potential persistent contrails using proxies and GAMs; $\log\left(\frac{p(X)}{1-p(X)}\right) =$		ETS
GAM <sub>0</sub>	$\beta_0 + s(RHi_{ERA5})$	0.337
GAM <sub>1</sub>	$\beta_0 + s(T) + s(RHi_{ERA5})$	0.372
GAM <sub>2</sub>	$\beta_0 + s(PV) + s(T) + s(RHi_{ERA5})$	0.372
GAM <sub>3</sub>	$\beta_0 + s(PV) + s(T) + s(\zeta) + s(RHi_{ERA5})$	0.373
GAM <sub>4</sub>	$\beta_0 + s(\gamma) + s(T) + s(Z) + s(PV) + s(\zeta)$	0.197
GAM <sub>5</sub>	$\beta_0 + s(\gamma) + s(T) + s(Z) + s(PV) + s(\zeta) + s(RHi_{ERA5})$	0.378

**Figure 3.** Conditional probability density functions  $f(r|ISS, a)$  (blue) and  $f(r|\overline{ISS}, a)$  (red) for different values of  $a$ . Note that the original distributions  $f_{RHi_{ERA5}}(r|\overline{ISS})$  and  $f_{RHi_{ERA5}}(r|ISS)$  are retained with  $a = 0.0$  in panel (f).**Figure 4.** Illustration of quantile mapping for  $RHi_{ERA5}$ . The red curve illustrates the cumulative distribution function (CDF) of  $RHi_{ERA5}$  and the blue one the CDF of  $RHi_{M/I}$ .

#### 4.2.2 $RHi$ modification by Teoh et al. (2022)

In a study by Teoh et al. (2022), the ERA5 ice supersaturation over the North Atlantic was adjusted to the corresponding MOZAIC/IAGOS supersaturation by introducing two factors used to scale  $RHi_{ERA5}$ :

$$RHi_{TEOH} = \frac{RHi_{ERA5}}{a} \quad \text{if} \quad \frac{RHi_{ERA5}}{a} \leq 1,$$

$$RHi_{TEOH} = \min \left[ \left( \frac{RHi_{ERA5}}{a} \right)^b, 1.65 \right] \quad \text{if} \quad \frac{RHi_{ERA5}}{a} > 1, \quad (9)$$

with  $a = 0.9779$  and  $b = 1.635$ . Here we test whether this modification can lead to improvements in our regression models.

**Table 5.** Results of the sensitivity test.

$\alpha$	1.0	0.9	0.8	0.7	0.6	0.5	0.4	0.3	0.2	0.1	0.0
ETS	1.0	0.996	0.989	0.976	0.956	0.921	0.863	0.765	0.639	0.484	0.372

#### 4.2.3 Results using corrections

Table 6 shows the results of comparing the observed ice supersaturation  $RHi_{M/I}$  with the modified relative humidities with respect to ice,  $RHi_{QM}$  and  $RHi_{TEOH}$ , and the results of using these corrected humidities in the best GAM we have found before (see Sect. 3.2.4). To recall the results to be compared, which we have already described, the ETS of the comparison of  $RHi_{ERA5}$  and  $RHi_{M/I}$  and also the original  $GAM_5$  have been added to the table.

We check how good the prediction of ice supersaturation is using the corrected versions of  $RHi_{ERA5}$ . When comparing the data of  $RHi_{M/I}$  with the modified relative humidity with respect to ice using the quantile mapping method,  $RHi_{QM}$ , the ETS reaches a value of 0.344. If the relative humidity with respect to ice is modified according to the formula of Teoh  $RHi_{TEOH}$  and compared to  $RHi_{M/I}$ , then the ETS is 0.284.

Now, we use the same proxies as in  $GAM_5$  but we replace  $RHi_{ERA5}$  with  $RHi_{QM}$  gained by quantile mapping and for the other case with  $RHi_{TEOH}$  using the formula by Teoh. The relative humidity of the whole data set is adapted. When  $RHi_{ERA5}$  is modified by quantile mapping, we get an ETS value of 0.377, and for a change in humidity, according to Teoh, the ETS value is 0.376.

Unfortunately, it turns out that neither a GAM produced with quantile-mapped ERA5 humidity values nor a GAM where the Teoh et al. (2022) corrections have been applied leads to larger ETS values than a GAM without the corrections (reminder that the ETS of the original  $GAM_5$  with the original  $RHi_{ERA5}$  is 0.378). In comparison to the ETS of 0.344 (quantile mapping) and 0.284 (Teoh) mentioned above, when only the modified humidities are compared with  $RHi_{M/I}$ , the GAMs with the best-suited proxies and the modified humidities hardly affect the ETS values.

The probable reason for this negative result is seen in Fig. 5, which shows the original conditional PDFs (red and blue) together with those obtained when the corrections are applied. Evidently, there is some shift for the PDFs conditioned on ISS in particular, but the overlap between the distribution pairs still remains considerable, that is, too substantial for a better result.

Another reason for the insensitivity of the GAMs to these corrections may be that they absorb such modifications in the coefficients of the non-linear smooth functions. This may become clearer if one thinks of a linear regression ( $Y = \beta_0 + \beta_1 X + \varepsilon$ ) where a linear correction of the predictor  $X$ , that is,  $X' = a + bX$ , would also simply be absorbed in the

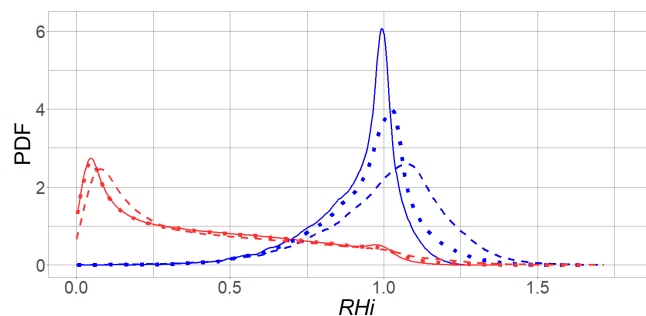


**Figure 5.** The conditioned PDFs  $P(RHi|ISS)$  (blue) and  $P(RHi|\overline{ISS})$  (red) of different  $RHi$  distributions are shown. The solid curves are the PDFs of the original  $RHi_{ERA5}$  of the whole data set for  $\overline{ISS}$  and  $ISS$ . The other curves represent  $RHi$  corrections: the dashed lines are the conditioned PDFs of  $RHi_{QM}$  modified by the quantile mapping method. The dotted curves represent the conditioned PDFs of  $RHi_{TEOH}$  modified by the Teoh formula.

regression coefficients  $\beta_0$  and  $\beta_1$ . That is, they would simply take different values, but the form of the regression and the ETS would not change.

## 5 Summary and conclusions

There are various approaches to minimising the climate impact of aviation. One of these approaches is to prevent the formation of persistent contrails by avoiding flying through ice-supersaturated regions, where contrails can last for hours. For implementing such aircraft diversions, these regions have to be accurately predicted in terms of time and location, which is currently associated with difficulties and uncertainties. This is mainly due to the inaccurate forecast of the relative humidity. Since ice supersaturation (ISS) is more common in some dynamical regimes than in others, we use different dynamical proxies (in addition to the relative humidity with respect to ice  $RHi_{ERA5}$  and to the temperature  $T$ ) as inputs to various approaches and methods to improve the prediction of these regions. These methods include a Bayesian approach and different regression models. The data of the variables/proxies come from ERA5, and the observation comes from MOZAIC/IAGOS, which we assume as the truth. With the data of MOZAIC/IAGOS, we can make the distinction between  $ISS$  and  $\overline{ISS}$ . The evaluation of the different methods is carried out with a score value (ETS) that checks how well the prediction matches the observation.

To find out which dynamical variables are best suited for the regressions and which do not provide redundant informa-

**Table 6.** Results of comparing  $RHi_{M/I}$  and the modified humidities,  $RHi_{QM}$  and  $RHi_{TEOH}$ , and of GAMs using  $RHi_{QM}$  and  $RHi_{TEOH}$ .

Comparison of raw data (assessment of the ISS-prediction without using a GAM)		ETS
	$RHi_{ERA5}$ and $RHi_{M/I}$	0.198
	$RHi_{QM}$ and $RHi_{M/I}$	0.344
	$RHi_{TEOH}$ and $RHi_{M/I}$	0.284
Prediction of potential persistent contrails using proxies and GAMs; $\log\left(\frac{p(X)}{1-p(X)}\right) =$		ETS
GAM <sub>5</sub>	$\beta_0 + s(\gamma) + s(T) + s(Z) + s(PV) + s(\zeta) + s(RHi_{ERA5})$	0.378
GAM <sub>5,QM</sub>	$\beta_0 + s(\gamma) + s(T) + s(Z) + s(PV) + s(\zeta) + s(RHi_{QM})$	0.377
GAM <sub>5,TEOH</sub>	$\beta_0 + s(\gamma) + s(T) + s(Z) + s(PV) + s(\zeta) + s(RHi_{TEOH})$	0.376

tion, we use various methods of information theory and test them. These include the log-likelihood ratios, known from Bayes' theorem; a modified form of the Kullback–Leibler divergence, which we call the expectation of the absolute logit; and the mutual information.

Log-likelihood ratios with values greater than 2 indicate that ISS is more likely than  $\overline{ISS}$ . Only  $RHi_{ERA5}$  delivers values above 2 in a larger range, which indicates that ISS is more likely there than  $\overline{ISS}$ . The vertical velocity,  $\omega$ , and the relative vorticity,  $\zeta$ , also show values above 2 but in a very small range. All other log-likelihood ratios are always below 2, which means that their effect on updating the prior odds ratio is quite small.

Particularly high values of the expectation for absolute logits are found for  $RHi_{ERA5}$ ; the lapse rate,  $\gamma$ ; and the relative vorticity,  $\zeta$ , which means that these proxies have the greatest learning effect when assessing whether the situation is ISS or  $\overline{ISS}$ .

Furthermore, to estimate the suitability of a proxy for a regression, we use the mutual information, which is a measure of how much information one variable,  $X$ , can provide about another variable,  $Y$ . To be a good predictor of ISS, it is important that the variable is both very well correlated with the relative humidity of the MOZAIC/IAGOS data,  $RHi_{M/I}$  (which we assume as the truth), and at the same time as uncorrelated as possible with the other variables.  $RHi_{ERA5}$ , PV,  $\gamma$ , and  $\zeta$  have the highest mutual information on  $RHi_{M/I}$ , but PV and  $\gamma$  are themselves especially quite strongly correlated, so it is sufficient for a regression to use PV and omit  $\gamma$  because of the higher mutual information of PV with  $RHi_{M/I}$ .

We use the most promising variables in several regression models to predict ISS. Through the regressions we find out that no matter which and how many dynamical proxies are added as an input, they provide only little new information regarding ISS. With only the raw  $RHi_{ERA5}$  and  $T$  data of ERA5, Gierens et al. (2020) could achieve an ETS value of 0.08 for the prediction of ice supersaturation. For the present data set, it is 0.198. The best regression that we can find achieves an ETS of 0.378. We consider this not satisfying for flight routing.

It turns out that the dynamical proxies hardly provide information on the question of whether a situation is ISS or  $\overline{ISS}$ , although the mutual information between  $RHi_{ERA5}$  and  $RHi_{M/I}$  and between PV and  $RHi_{M/I}$  in particular is quite large. Furthermore, we see that, of all variables, only  $RHi_{ERA5}$  has a range of values with the logit function exceeding the critical level of 2 and that a regression without  $RHi_{ERA5}$  is not successful. Thus, it turns out that the relative humidity,  $RHi_{ERA5}$ , at flight level is essential in our regressions in spite of its weaknesses. We suspect that the main problem with predicting ISS is the strong overlap of the conditional probability density functions  $P(RHi_{ERA5}|ISS)$  and  $P(RHi_{ERA5}|\overline{ISS})$ , especially in the critical region around  $RHi_{ERA5}$  of 70% to 100%. Sensitivity tests show that the ETS increases strongly with a decrease in the overlap, which means that if  $P(RHi_{ERA5}|ISS)$  and  $P(RHi_{ERA5}|\overline{ISS})$  were just slightly more separated, the results would drastically improve. While corrections of  $RHi_{ERA5}$  lead to better predictions of ice supersaturation (increase in the ETS values) for comparing  $RHi_{M/I}$  with the modified relative humidities, they only slightly improve the forecast of potential persistent contrails (based on the ETS of the ISS prediction) using regression methods, the proxies that turned out to be the most suitable ones, and the modified relative humidities. This is due to the fact that the overlap of the conditional PDFs  $P(RHi|ISS)$  and  $P(RHi|\overline{ISS})$  of the modified relative humidities is also hardly reduced and probably also because the corrections are absorbed by the regressions, and thus they do not become effective.

In the present paper, we use the meteorological data only at the point and time where the prediction of ice supersaturation is required. One can increase the effort and use additional forecast data from earlier points in time and locations upstream of the location of interest (e.g. Duda and Minnis, 2009a, b). Wang et al. (2024) report that the humidity forecast of the ECMWF model can be improved by the application of an artificial neural network fed with data from previous atmospheric states (a couple of hours) and covering about 100 hPa in vertical distance in order to account for the past vertical motion that led to the current state. While this is certainly a possibility when it comes to improving the predicted

humidity field per se, it is not clear whether the methods are fast and accurate enough for flight planning. Duda and Minnis (2009b) conclude that “reductions in the uncertainties of meteorological variables to a point where acceptable contrail forecasts are produced would be a good goal for NWA [numerical weather analysis] modelers”.

We conclude that the representation of RH<sub>i</sub> in models of numerical weather prediction needs to be improved. There are several ways to do this, but it will take some time to realise any of them. Cloud physics in numerical weather models is greatly simplified. This was justified for a long time because of the constraints of computing time and because the processes at flight level were not the focus of weather prediction. However, as aviation needs to reduce its climate impact, avoidance of contrails gets interesting for airlines and thus the prediction of ice supersaturation needs improvement. Furthermore, computer power is rising and additional resources can be used to improve the description of physical processes. A recent example is the concept of a one-moment scheme by Sperber and Gierens (2023). Furthermore, we think that more aircraft need to be equipped with hygrometers to measure humidity at flight altitudes for data assimilation. This would enable numerical weather models to improve the prediction of relative humidity for flight routing.

**Code availability.** R codes can be shared on request.

**Data availability.** ERA5 data can be obtained from the Copernicus Climate Data Service at <https://cds.climate.copernicus.eu> (Hersbach et al., 2023). MOZAIC/IAGOS data are available from <https://iagos.aeris-data.fr> (IAGOS, 2024).

**Author contributions.** This paper is part of SH’s PhD thesis. SH wrote the codes, ran the calculations, analysed the results, and produced the figures. KG supervised her research. SH and KG discussed the methods and results and wrote the paper. SR curated the MOZAIC/IAGOS data.

**Competing interests.** The contact author has declared that none of the authors has any competing interests.

**Disclaimer.** Publisher’s note: Copernicus Publications remains neutral with regard to jurisdictional claims made in the text, published maps, institutional affiliations, or any other geographical representation in this paper. While Copernicus Publications makes every effort to include appropriate place names, the final responsibility lies with the authors.

**Acknowledgements.** The authors would like to thank Robert Sausen for the helpful discussion and Johanna Mayer

for her thorough read-through and comments on a draft of the paper.

**Financial support.** This research has been supported by the Horizon 2020 Framework Programme H2020 Societal Challenges as part of project ACACIA (grant no. 875036).

The article processing charges for this open-access publication were covered by the German Aerospace Center (DLR).

**Review statement.** This paper was edited by Fangqun Yu and reviewed by two anonymous referees.

## References

- Appleman, H.: The formation of exhaust condensation trails by jet aircraft, *Bull. Am. Meteorol. Soc.*, 34, 14–20, 1953.
- Copernicus Climate Change Service (C3S): ERA5: Fifth generation of ECMWF atmospheric reanalyses of the global climate, Copernicus Climate Change Service Climate Data Store (CDS), <https://cds.climate.copernicus.eu/cdsapp#!/home> (last access: 4 July 2024), 2017.
- Corti, T. and Peter, T.: A simple model for cloud radiative forcing, *Atmos. Chem. Phys.*, 9, 5751–5758, <https://doi.org/10.5194/acp-9-5751-2009>, 2009.
- Duda, D. and Minnis, P.: Basic Diagnosis and Prediction of Persistent Contrail Occurrence Using High-Resolution Numerical Weather Analyses/Forecasts and Logistic Regression, Part I: Effects of Random Error, *J. Appl. Meteorol. Clim.*, 48, 1780–1789, 2009a.
- Duda, D. and Minnis, P.: Basic Diagnosis and Prediction of Persistent Contrail Occurrence Using High-Resolution Numerical Weather Analyses/Forecasts and Logistic Regression, Part II: Evaluation of Sample Models, *J. Appl. Meteorol. Clim.*, 48, 1790–1802, 2009b.
- ERA5: ERA5 data, <https://cds.climate.copernicus.eu> (last access: 4 July 2024), 2024.
- Gierens, K. and Brinkop, S.: Dynamical characteristics of ice supersaturated regions, *Atmos. Chem. Phys.*, 12, 11933–11942, <https://doi.org/10.5194/acp-12-11933-2012>, 2012.
- Gierens, K. and Eleftheratos, K.: Technical note: On the intercalibration of HIRS channel 12 brightness temperatures following the transition from HIRS 2 to HIRS 3/4 for ice saturation studies, *Atmos. Meas. Tech.*, 10, 681–693, <https://doi.org/10.5194/amt-10-681-2017>, 2017.
- Gierens, K. and Eleftheratos, K.: The contribution and weighting functions of radiative transfer – theory and application to the retrieval of upper-tropospheric humidity, *Meteorol. Z.*, 30, 79–88, <https://doi.org/10.1127/metz/2020/0985>, 2020.
- Gierens, K., Matthes, S., and Rohs, S.: How well can persistent contrails be predicted?, *Aerospace*, 7, 169, <https://doi.org/10.3390/aerospace7120169>, 2020.
- Gierens, K., Wilhelm, L., Hofer, S., and Rohs, S.: The effect of ice supersaturation and thin cirrus on lapse rates in the upper troposphere, *Atmos. Chem. Phys.*, 22, 7699–7712, <https://doi.org/10.5194/acp-22-7699-2022>, 2022.

- Hersbach, H., Bell, B., Berrisford, P., Biavati, G., Horányi, A., Muñoz Sabater, J., Nicolas, J., Peubey, C., Radu, R., Rozum, I., Schepers, D., Simmons, A., Soci, C., Dee, D., and Thépaut, J.-N.: ERA5 hourly data on single levels from 1979 to present, Tech. Rep., Copernicus Climate Change Service (C3S) Climate Data Store (CDS), <https://doi.org/10.24381/cds.adbb2d47>, 2018a.
- Hersbach, H., Bell, B., Berrisford, P., Biavati, G., Horányi, A., Muñoz Sabater, J., Nicolas, J., Peubey, C., Radu, R., Rozum, I., Schepers, D., Simmons, A., Soci, C., Dee, D., and Thépaut, J.-N.: ERA5 hourly data on pressure levels from 1979 to present, Tech. Rep., Copernicus Climate Change Service (C3S) Climate Data Store (CDS), <https://doi.org/10.24381/cds.bd0915c6>, 2018b.
- Hersbach, H., Bell, B., Berrisford, P., Hirahara, S., Horányi, A., Muñoz Sabater, J., Nicolas, J., Peubey, C., Radu, R., Schepers, D., Simmons, A., Soci, C., Abdalla, S., Abellan, X., Balsamo, G., Bechtold, P., Biavati, G., Bidlot, J., Bonavita, M., De Chiara, G., Dahlgren, P., Dee, D., Diamantakis, M., Dragani, R., Flemming, J., Forbes, R., Fuentes, M., Geer, A., Haimberger, L., Healy, S., Hogan, R. J., Hólm, E., Janisková, M., Keeley, S., Laloyaux, P., Lopez, P., Lupu, C., Radnoti, G., de Rosnay, P., Rozum, I., Vamborg, F., Villaume, S., and Thépaut, J.-N.: The ERA5 global reanalysis, *Q. J. Roy. Meteorol. Soc.*, 146, 1999–2049, <https://doi.org/10.1002/qj.3803>, 2020.
- Hersbach, H., Bell, B., Berrisford, P., Biavati, G., Horányi, A., Muñoz Sabater, J., Nicolas, J., Peubey, C., Radu, R., Rozum, I., Schepers, D., Simmons, A., Soci, C., Dee, D., and Thépaut, J.-N.: ERA5 hourly data on pressure levels from 1940 to present, Copernicus Climate Change Service (C3S) Climate Data Store (CDS) [data set], <https://doi.org/10.24381/cds.bd0915c6>, 2023.
- IAGOS: IAGOS-Core data [data set], <http://www.iagos.org/> (last access: 4 July 2024), 2024.
- Ihaka, R. and Gentleman, R.: The R Project for Statistical Computing, The R Project for Statistical Computing, <https://www.r-project.org/> (last access: 4 July 2024), 1993.
- Marengo, A., Thouret, V., Nedelec, P., Smit, H., Helten, M., Kley, D., Karcher, F., Simon, P., Law, K., Pyle, J., Poschmann, G., Wrede, R. V., Hume, C., and Cook, T.: Measurement of ozone and water vapor by Airbus in-service aircraft: The MOZAIK airborne program, An overview, *J. Geophys. Res.*, 103, 25631–25642, 1998.
- Neis, P.: Water vapour in the UTLS – climatologies and transport, Ph.D. thesis, Johannes Gutenberg-Universität Mainz, Germany, Schriften des Forschungszentrums Jülich Reihe Energie and Umwelt/Energy and Environment, ISBN: 978-3-95806-269-6, 2017.
- Petzold, A., Thouret, V., Gerbig, C., Zahn, A., Brenninkmeijer, C., Gallagher, M., Hermann, M., Pontaud, M., Ziereis, H., Boulanger, D., Marshall, J., Nedelec, P., Smit, H., Friess, U., Flaud, J.-M., Wahner, A., Cammas, J.-P., and Volz-Thomas, A.: Global-scale atmosphere monitoring by in-service aircraft – current achievements and future prospects of the European Research Infrastructure IAGOS, *Tellus B*, 67, 28452, <https://doi.org/10.3402/tellusb.v67.28452>, 2015.
- Petzold, A., Neis, P., Rütimann, M., Rohs, S., Berkes, F., Smit, H., Krämer, M., Spelten, N., Spichtinger, P., Nedelec, P., and Wahner, A.: Ice-supersaturated air masses in the northern mid-latitudes from regular in situ observations by passenger aircraft: vertical distribution, seasonality and tropospheric fingerprint, *Atmos. Chem. Phys.*, 20, 8157–8179, <https://doi.org/10.5194/acp-20-8157-2020>, 2020.
- Rädler, A., Groenemeijer, P., Faust, E., and Sausen, R.: Detecting Severe Weather Trends Using an Additive Regressive Convective Hazard Model (AR-CHaMo), *J. Appl. Meteorol. Clim.*, 57, 569–587, 2018.
- Schmidt, E.: Die Entstehung von Eisnebel aus den Auspuffgasen von Flugmotoren, *Schr. Deut. Akad. Luftf.*, 44, 1–15, 1941.
- Schumann, U.: On conditions for contrail formation from aircraft exhausts, *Meteorol. Z.*, 5, 4–23, 1996.
- Schumann, U., Mayer, B., Graf, K., and Mannstein, H.: A parametric radiative forcing model for contrail cirrus, *J. Appl. Meteorol. Climatol.*, 51, 1391–1406, 2012.
- Sperber, D. and Gierens, K.: Towards a more reliable forecast of ice supersaturation: Concept of a one-moment ice cloud scheme that avoids saturation adjustment, *Atmos. Chem. Phys.*, 23, 15609–15627, <https://doi.org/10.5194/acp-23-15609-2023>, 2023.
- Teoh, R., Schumann, U., Majumdar, A., and Stettler, M.: Mitigating the climate forcing of aircraft contrails by small-scale diversions and technology adoption, *Environ. Sci. Technol.*, 54, 2941–2950, <https://doi.org/10.1021/acs.est.9b05608>, 2020.
- Teoh, R., Schumann, U., Gryspeerd, E., Shapiro, M., Molloy, J., Koudis, G., Voigt, C., and Stettler, M.: Aviation contrail climate effects in the North Atlantic from 2016 to 2021, *Atmos. Chem. Phys.*, 22, 10919–10935, <https://doi.org/10.5194/acp-22-10919-2022>, 2022.
- Tompkins, A., Gierens, K., and Rädler, G.: Ice supersaturation in the ECMWF Integrated Forecast System, *Quart. J. Roy. Met. Soc.*, 133, 53–63, 2007.
- Voigt, C., Schumann, U., Minikin, A., Abdelmonem, A., Afchine, A., Borrmann, S., Boettcher, M., Buchholz, B., Bugliaro, L., Costa, A., Curtius, J., Dollner, M., Dörnbrack, A., Dreiling, V., Ebert, V., Ehrlich, A., Fix, A., Forster, L., Frank, F., Fütterer, D., Giez, A., Graf, K., Groß, J.-U., Groß, S. M., Heimerl, K., Heinold, B., Hüneke, T., Järvinen, E., Jurkat, T., Kaufmann, S., Kenntner, M., Klingebiel, M., Klimach, T., Kohl, R., Krämer, M., Krisna, T. C., Luebke, A., Mayer, B., Mertes, S., Molleker, S., Petzold, A., Pfeilsticker, K., Port, M., Rapp, M., Reutter, P., Rolf, C., Rose, D., Sauer, D., Schäfer, A., Schlage, R., Schnaiter, M., Schneider, J., Spelten, N., Spichtinger, P., Stock, P., Walser, A., Weigel, R., Weinzierl, B., Wendisch, M., Werner, F., Wernli, H., Wirth, M., Zahn, A., Ziereis, H., and Zöger, M.: ML-CIRRUS: The Airborne Experiment on Natural Cirrus and Contrail Cirrus with the High-Altitude Long-Range Research Aircraft HALO, *Bull. Am. Meteorol. Soc.*, 98, 271–288, 2017.
- Wang, Z., Bugliaro, L., Gierens, K., Hegglin, M. I., Rohs, S., Petzold, A., Kaufmann, S., and Voigt, C.: Machine learning for improvement of upper tropospheric relative humidity in ERA5 weather model data, preprint, 2024.
- Wilhelm, L., Gierens, K., and Rohs, S.: Meteorological conditions that promote persistent contrails, *Appl. Sci.*, 12, 4450, <https://doi.org/10.3390/app12094450>, 2022.
- Wilson, D. and Ballard, S.: A microphysically based precipitation scheme for the UK meteorological office unified model, *Q. J. Roy. Meteorol. Soc.*, 125, 1607–1636, <https://doi.org/10.1002/qj.49712555707>, 1999.
- Wolf, K., Bellouin, N., and Boucher, O.: Sensitivity of cirrus and contrail radiative effect on cloud microphysical and envi-

ronmental parameters, *Atmos. Chem. Phys.*, 23, 14003–14037, <https://doi.org/10.5194/acp-23-14003-2023>, 2023a.

Wolf, K., Bellouin, N., Boucher, O., Rohs, S., and Li, Y.: Correction of temperature and relative humidity biases in ERA5 by bivariate quantile mapping: Implications for contrail classification, *EGU-sphere* [preprint], <https://doi.org/10.5194/egusphere-2023-2356>, 2023b.